

# Ionothermal Synthesis of Hierarchical ZnO Nanostructures from Ionic-Liquid Precursors

Haoguo Zhu, Jing-Fang Huang, Zhengwei Pan, and Sheng Dai\*

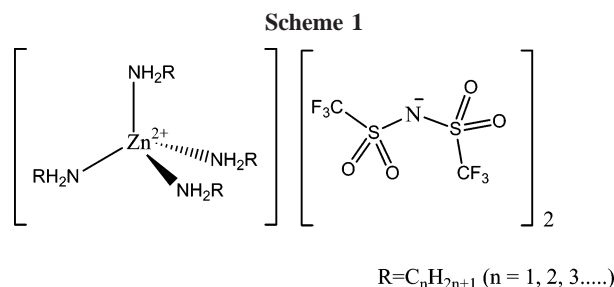
Chemical Sciences Division, Oak Ridge National Laboratory, Oak Ridge, Tennessee 37831

Received February 26, 2006. Revised Manuscript Received July 12, 2006

An ionothermal process was employed to synthesize the hierarchical structures of zinc oxide with diverse morphologies. The key to this synthesis methodology was the use of metal-containing ionic liquids that acted both as solvents and as metal precursors in the ionothermal process. The growth environment was highly homogeneous, allowing facile control over reaction conditions. The morphologies of zinc oxide were strongly dependent on the nature of the corresponding ionic-liquid precursors, providing unique methodologies to control growth conditions.

## Introduction

Ionic liquids (ILs) are being actively investigated as alternative solvent media in synthesis, catalysis, separation, and electrochemistry.<sup>1–8</sup> These solvent systems can offer a novel chemical environment that can uniquely influence the course of chemical reactions as compared to those in traditional solvents. Recently, ILs have also attracted the attention of the inorganic materials community because of their unique properties, such as negligible vapor pressure, thermal stability, high polarity, etc.<sup>3,9–11</sup> ILs have been demonstrated to be not only functional solvents for reaction precursors but also morphologic templates for porous materials.<sup>9,10,12</sup> This dual functionality enables the synthesis of inorganic materials with novel and improved properties.<sup>13–16</sup> Accordingly, ionic liquids can be promising “all-in-one” solvents for synthesis of inorganic materials.<sup>10</sup> For example, Cooper et al.<sup>11</sup> have recently demonstrated that imidazolium-based ionic liquids can be utilized to synthesize several



phosphate-based microporous zeolites. The syntheses hinge on the solvents being predominantly ionic. This thermal reaction using ionic liquids as reaction media was termed as an “ionothermal” process to distinguish it from hydrothermal methods, which take place in a predominantly molecular solvent.<sup>11</sup> Herein, we report the use of a newly developed ionic-liquid system containing zinc metal ions,<sup>17</sup> which can serve as both solvents and metal-oxide precursors, for manufacturing nanostructured zinc oxide under the ionothermal condition. The general structural feature of these new ILs is given in Scheme 1.

Our strategy to tailor the morphology and orientation of ZnO crystallites consists of both thermodynamic and kinetic control over the nucleation and growth of metal-oxide materials in “supramolecular” IL solvents.<sup>10</sup> Both chemical composition and electrostatic interactions can be tailored via strategic choice of ligands and metal ions. The synthesis conditions were tuned to allow the thermolysis of a cationic zinc alkylamine-derived complex precursor in ILs under basic conditions. The nucleation kinetic processes were regulated by adjusting both temperature and concentration of the reaction precursors.<sup>18</sup> The uniform and hierarchical structures were assembled from zinc oxide nanocrystals.

Zinc oxide (ZnO), which exhibits a wide range of technological applications, including the applications as transparent conducting electrodes for solar cells, flat panel

- \* To whom all correspondence should be addressed. E-mail: dais@ornl.gov.
- (1) Dupont, J.; de Souza, R. F.; Suarez, P. A. Z. *Chem. Rev.* **2002**, *102*, 3667–3691.
  - (2) Buzzeo, M. C.; Evans, R. G.; Compton, R. G. *ChemPhysChem* **2004**, *5*, 1107–1120.
  - (3) Brennecke, J. F.; Maginn, E. J. *AIChE J.* **2001**, *47*, 2384–2389.
  - (4) Huddleston, J. G.; Willauer, H. D.; Swatloski, R. P.; Visser, A. E.; Rogers, R. D. *Chem. Commun.* **1998**, 1765–1766.
  - (5) Dai, S.; Ju, Y. H.; Barnes, C. E. *J. Chem. Soc., Dalton Trans.* **1999**, 1201–1202.
  - (6) Visser, A. E.; Swatloski, R. P.; Reichert, W. M.; Mayton, R.; Sheff, S.; Wierzbicki, A.; Davis, J. H.; Rogers, R. D. *Chem. Commun.* **2001**, 135–136.
  - (7) Seddon, K. R. *Nat. Mater.* **2003**, *2*, 363–365.
  - (8) Wasserscheid, P.; Keim, W. *Angew. Chem., Int. Ed.* **2000**, *39*, 3773–3789.
  - (9) Dai, S.; Ju, Y. H.; Gao, H. J.; Lin, J. S.; Pennycook, S. J.; Barnes, C. E. *Chem. Commun.* **2000**, 243–244.
  - (10) Antonietti, M.; Kuang, D. B.; Smarsly, B.; Yong, Z. *Angew. Chem., Int. Ed.* **2004**, *43*, 4988–4992.
  - (11) Cooper, E. R.; Andrews, C. D.; Wheatley, P. S.; Webb, P. B.; Wormald, P.; Morris, R. E. *Nature* **2004**, *430*, 1012–1016.
  - (12) Nakashima, T.; Kimizuka, N. *J. Am. Chem. Soc.* **2003**, *125*, 6386–6387.
  - (13) Taubert, A. *Angew. Chem., Int. Ed.* **2004**, *43*, 5380–5382.
  - (14) Zhu, Y. J.; Wang, W. W.; Qi, R. J.; Hu, X. L. *Angew. Chem., Int. Ed.* **2004**, *43*, 1410–1414.
  - (15) Zhou, Y.; Antonietti, M. *J. Am. Chem. Soc.* **2003**, *125*, 14960–14961.
  - (16) Zhou, Y.; Antonietti, M. *Chem. Mater.* **2004**, *16*, 544–550.

- (17) Huang, J. F.; Luo, H. M.; Dai, S. J. *Electrochem. Soc.* **2006**, *153*, J9–J13.
- (18) Vayssieres, L.; Graetzel, M. *Angew. Chem., Int. Ed.* **2004**, *43*, 3666–3670.

displays, surface acoustic wave devices, and chemical sensors, is a potentially useful semiconductor with a direct band gap of 3.37 eV. The properties of ZnO depend highly on its nanostructures, including crystal sizes, orientations, morphologies, aspect ratios, and even crystalline densities. Both surface structures and morphologies also play a crucial role in many applications (e.g., photoemitters, transducers, actuators, sensors, and catalysts).<sup>19–22</sup> Since Yang et al. have reported the synthesis of ZnO nanowire arrays,<sup>23</sup> various techniques have been developed to synthesize ZnO with controlled nanostructures.<sup>24</sup> Many interesting structures of ZnO, including nanobelts, nanobridges, and nanorings, have been fabricated by thermal evaporation of oxide powders.<sup>25–29</sup> Recently, ZnO microstructures have also been successfully prepared through both aqueous phase and gas phase reactions.<sup>24,30–33</sup> The ionothermal process reported here offers a unique alternative in synthesizing highly uniform and hierarchical ZnO structures.

## Experimental Section

**1. Preparation of ILs Based on Complexes of Zinc Ions.** In a typical synthesis,<sup>17</sup> an excess amount of a selected alkylamine ligand ( $\text{H}_2\text{N}-\text{R}$ , neutral organic ligand) was added dropwise to an aqueous solution of  $\text{Zn}(\text{NO})_2 \cdot 2\text{H}_2\text{O}$ . The mole ratio of zinc to amine is about 6. A white precipitate was initially produced. Subsequently, the resulting cloudy solution became clear after the completion of the complexation reaction between alkylamine ligands and zinc ions. Because the formation constant of zinc-hydroxide complexes is higher than those of zinc-alkylamine complexes,<sup>17</sup> the addition of an excess amount of alkylamine is required to dissolve the white hydroxide precipitate for formation of the transparent aqueous solution containing the corresponding zinc-alkylamine complexes. The aqueous solution containing  $\text{Zn}(\text{H}_2\text{N}-\text{R})_4^{2+}$  was mixed with the solution containing  $\text{LiTf}_2\text{N}$  ( $\text{NTf}_2^- = ^-\text{N}(\text{SO}_2\text{CF}_3)_2$ ). The mole ratio of  $\text{Zn}^{2+}$  to  $\text{Tf}_2\text{N}^-$  is 0.5. The biphasic solution system was obtained. The lower layer contained the hydrophobic IL of  $\text{Zn}(\text{H}_2\text{N}-\text{R})_4^{2+} (\text{Tf}_2\text{N}^-)_2$ . The ionic-liquid phase was washed with D.I. water to ensure that all  $\text{LiNO}_3$  residues were removed. The removal of water and amine residues via rotary evaporation produced the desired IL, which, was further purified by vacuum-drying through

a mechanic pump equipped with a liquid-nitrogen trap. The elemental analysis for this ionic liquid from the butylamine ligand (C: 25.54, H: 4.82, N: 9.08, and Zn 6.50%) is consistent with the calculated value for  $\text{C}_{20}\text{H}_{44}\text{N}_6\text{O}_8\text{S}_4\text{F}_{12}\text{Zn}$  (C: 26.16, H: 4.83, N: 9.15, and Zn: 7.12%; elemental analysis was performed by Galbraith Laboratories Inc). This result supports that the composition of the zinc-containing ionic liquid is  $\text{Zn}(\text{H}_2\text{N}-\text{C}_4\text{H}_9)_4^{2+} (\text{Tf}_2\text{N}^-)_2$ . The water content of this ionic liquid from a Karl-Fisher titration is 287 ppm.

**2. Synthesis of the ZnO Superstructures.** In a typical run, 0.1 mL of tetramethylammonium hydroxide (25% in methanol) was slowly added to the above ionic liquid [1 mL,  $\text{Zn}(\text{L})_4(\text{NTf}_2)_2$  (L = alkylamine)] under stirring. The mixed solution was stirred for 10–30 min until it turned optically transparent. Subsequently, methanol was removed under vacuum at ambient temperature. The resulting solution was aging in an oven at a specific temperature (e.g. 110 °C) for several hours. The clear solution gradually became turbid. The ZnO product was collected with centrifugation and rinsed with ethanol.

**3. Characterization Techniques.** The powder X-ray diffraction patterns of the samples were recorded using a SIEMENS D5005 X-ray diffractometer, where a Cu target  $\text{K}\alpha$  ray ( $\lambda = 0.154$  nm) and operating at 40 kV and 40 mA) was used as an X-ray source. The morphology of the samples was examined by JEOL JSM-6060 scanning electron microscope (SEM). The microstructures of the samples were investigated with a Philips CM200 high-resolution TEM (HRTEM) operating at 200 kV. The water content was measured by a Metrohm 652 KF-coulometer.

## Results and Discussion

The ILs of  $\text{Zn}(\text{L})_4(\text{NTf}_2)_2$  [L = alkylamine,  $\text{NTf}_2^- = ^-\text{N}(\text{SO}_2\text{CF}_3)_2$ ] were all liquid at ambient temperature with exception of  $\text{Zn}(\text{CH}_3\text{NH}_2)_4(\text{NTf}_2)_2$  and  $\text{Zn}(\text{CH}_3\text{CH}_2\text{NH}_2)_4(\text{NTf}_2)_2$ . The melting points of the latter two ILs were about 40–50 °C. These metal-containing ILs were synthesized with a new synthesis strategy developed recently in our group.<sup>17</sup> The essence of this strategy is to form the cations of ionic liquids through the complexation reactions of neutral organic ligands with metal ions, followed by the metathesis reactions of the resulting salts with anion donors. These new ionic liquids have properties similar to those of the conventional ILs (e.g. high polarity, negligible vapor pressure, high ionic conductivity, and good thermal stability). The important advantage of these ILs, however, lies in the dual functionality that these ILs can act both as solvents and as metal-oxide precursors. The objective of our present work was to demonstrate a novel protocol to fabricate ZnO with a well-developed crystal habit and a tunable Abstract morphology under the ionothermal condition through the controlled introduction of hydroxide groups into the Zn-containing ILs for nucleation of zinc oxide.<sup>11</sup>

The prerequisite for the nucleation formation of ZnO was the addition of a small amount of tetramethylammonium hydroxide to the  $\text{Zn}(\text{L})_4(\text{NTf}_2)_2$  ILs ( $[\text{OH}]/\text{Zn} \approx 1/10$ ). The resulting solutions were clear at room temperature, indicating the high stability of the ILs against hydrolysis.<sup>17</sup> The hydrolysis-induced nucleation can be, however, readily initiated under the ionothermal condition. The induction time ranges from 10 min to several hours, depending on the nucleation temperature. The XRD pattern (Figure 1) of ZnO prepared at 110 °C can be indexed as a hexagonal wurtzite

- (19) Emanetoglu, N. W.; Gorla, C.; Liu, Y.; Liang, S.; Lu, Y. *Mater. Sci. Semicond. Process.* **1999**, *2*, 247–252.
- (20) Saito, N.; Haneda, H.; Sekiguchi, T.; Ohashi, N.; Sakaguchi, I.; Koumoto, K. *Adv. Mater.* **2002**, *14*, 418–421.
- (21) Lin, Y. H.; Zhang, Z. T.; Tang, Z. L.; Yuan, F. L.; Li, J. L. *Adv. Mater. Opt. Electron.* **1999**, *9*, 205–209.
- (22) Golego, N.; Studenikin, S. A.; Cocivera, M. *J. Electrochem. Soc.* **2000**, *147*, 1592–1594.
- (23) Huang, M. H.; Mao, S.; Feick, H.; Yan, H. Q.; Wu, Y. Y.; Kind, H.; Weber, E.; Russo, R.; Yang, P. D. *Science* **2001**, *292*, 1897–1899.
- (24) Vayssieres, L. *Adv. Mater.* **2003**, *15*, 464–466.
- (25) Pan, Z. W.; Dai, Z. R.; Wang, Z. L. *Science* **2001**, *291*, 1947–1949.
- (26) Kong, X. Y.; Wang, Z. L. *Nano Lett.* **2003**, *3*, 1625–1631.
- (27) Kong, X. Y.; Ding, Y.; Yang, R.; Wang, Z. L. *Science* **2004**, *303*, 1348–1351.
- (28) Pan, Z. W.; Mahurin, S. M.; Dai, S.; Lowndes, D. H. *Nano Lett.* **2005**, *5*, 723–727.
- (29) Pan, Z. W.; Dai, S.; Rouleau, C. M.; Lowndes, D. H. *Angew. Chem., Int. Ed.* **2005**, *44*, 274–278.
- (30) Tian, Z. R. R.; Voigt, J. A.; Liu, J.; McKenzie, B.; McDermott, M. J. *J. Am. Chem. Soc.* **2002**, *124*, 12954–12955.
- (31) Tian, Z. R. R.; Voigt, J. A.; Liu, J.; McKenzie, B.; McDermott, M. J.; Rodriguez, M. A.; Konishi, H.; Xu, H. F. *Nat. Mater.* **2003**, *2*, 821–826.
- (32) Chittofrati, A.; Matijevic, E. *Colloids Surf.* **1990**, *48*, 65–78.
- (33) Zhang, J.; Sun, L. D.; Yin, J. L.; Su, H. L.; Liao, C. S.; Yan, C. H. *Chem. Mater.* **2002**, *14*, 4172–4177.

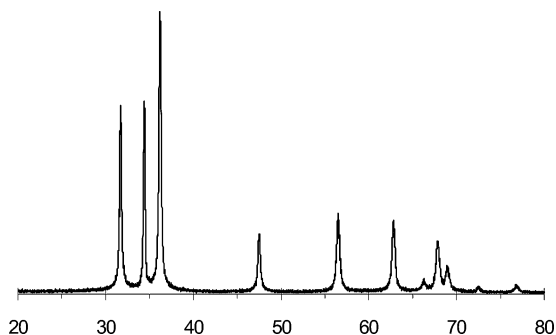


**Figure 1.** XRD pattern of ZnO synthesized using the IL containing zinc ions.

structure with the lattice constants in agreement with the values given in the commercial XRD database of JADE (Materials Data, Inc., Livermore, CA). Figure 2a shows the corresponding SEM images of the ZnO particles obtained from  $\text{Zn}(\text{CH}_3\text{NH}_2)_4(\text{NTf}_2)_2$ . The obtained spherical particles have a diameter ranging from 2 to 4  $\mu\text{m}$ . Each spherical particle is hierarchically structured and composed of hundreds of ZnO nanoplates with a uniform thickness of  $\sim 50$  nm. The typical lateral dimension of the nanoplates is between 0.5 and 1  $\mu\text{m}$ . Some nanoplates were connected at their junctions. The HRTEM image of the same sample indicates that the structure of the nanoplates is a single crystal, as shown in Figure 2b.

When methylamine in  $\text{Zn}(\text{CH}_3\text{NH}_2)_4(\text{NTf}_2)_2$  was replaced by ethylamine, a flowerlike morphology of ZnO (Figure 2c) was formed with an average size of 5  $\mu\text{m}$ . This morphology is different from those formed from aqueous solutions containing hexamethylenetetramine and zinc ions.<sup>33</sup> A hierarchical organization is clearly revealed in Figure 2c. The petals of the flowerlike structure are, in fact, derived from the bundling of one-dimensional nanostrips.<sup>34</sup> The nanostrips are aligned with one another along some main crystallographic axes of ZnO possibly by an oriented attachment process,<sup>35–37</sup> as shown in the inset in Figure 2c. The bundling of these nanostrips could lead to coalescence, forming a larger diameter rod. The HRTEM image further reveals the crystalline nature of a single nanostrip in Figure 2d. When propylamine was used as a ligand, a well-developed flowerlike morphology for ZnO was obtained, as shown in Figure 2e. The petals of the flowers stem from the individual nanocrystals based on the TEM image shown in Figure 2f. This texture is different from those in the petals of the flowerlike ZnO synthesized from  $\text{Zn}(\text{C}_2\text{H}_5\text{NH}_2)_4(\text{NTf}_2)_2$ . The electron-diffraction (ED) pattern (see the Supporting Information) indicates the crystalline nature of the sample and its hexagonal phase, which is also consistent with the results of XRD characterization. When butylamine was used as a ligand, the flowerlike ZnO morphology (Figure 2g) assembled from ZnO nanoparticles was also observed. With the increase of alkyl chains in  $\text{RNH}_2$  ligands, the petals of the flowerlike morphology change from tapering to oval features. When octylamine was used as ligands, the nano-

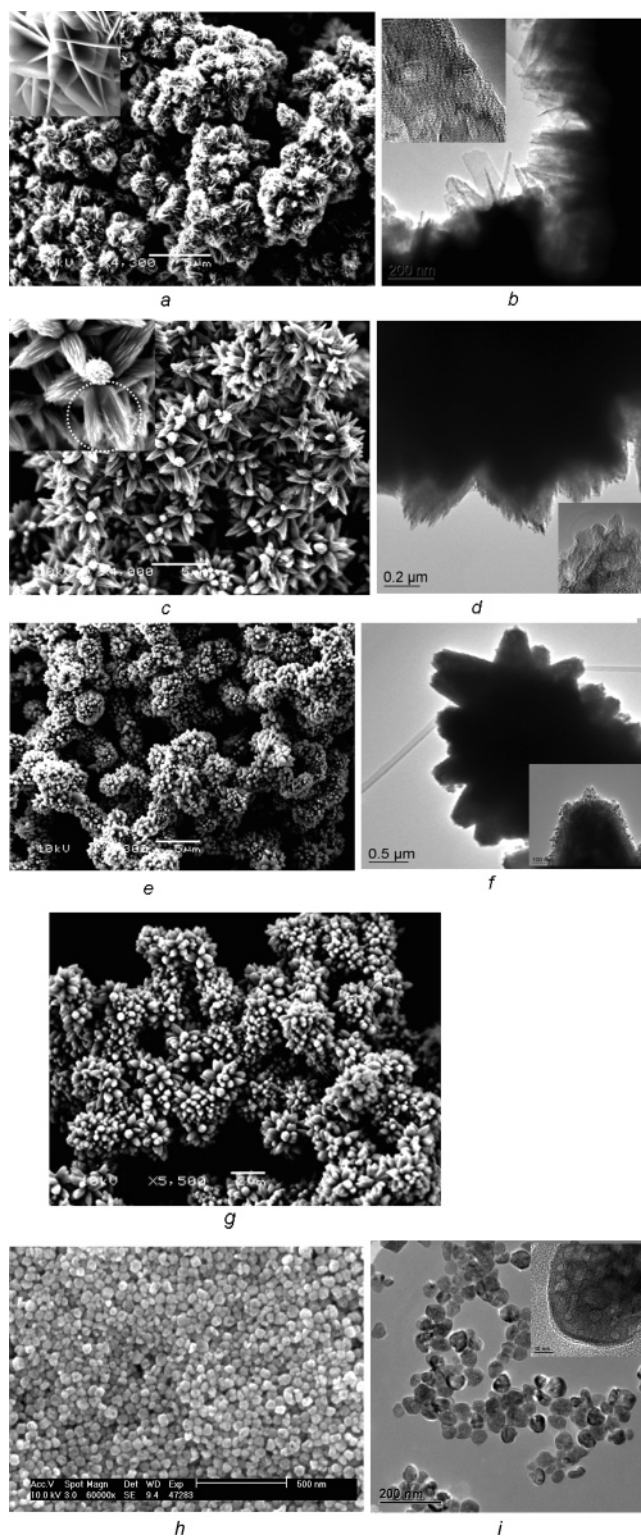


**Figure 2.** Representative SEM images of ZnO synthesized from the ILs containing different amine ligands at 110  $^{\circ}\text{C}$ : (a) L = methylamine, (c) L = ethylamine (a bundle has fused together to form a single petal in the upper left corner), (e) L = propylamine, (g) L = butylamine, and (h) L = octylamine. Representative TEM images and insets corresponding to (b) L = methylamine, (d) L = ethylamine, (f) L = propylamine, and (i) L = octylamine.

particles with diameters 60–70 nm were obtained, as shown in Figure 2h. These particles were not really spherical, and the TEM images of the particles were shown in Figure 2i. The homogeneous growth environment offered by the ILs leads to the large scale and uniform growth of ZnO.

(34) Li, Q. C.; Kumar, V.; Li, Y.; Zhang, H. T.; Marks, T. J.; Chang, R. P. H. *Chem. Mater.* **2005**, *17*, 1001–1006.

(35) Liu, B.; Zeng, H. C. *J. Am. Chem. Soc.* **2004**, *126*, 16744–16746.

(36) Penn, R. L.; Banfield, J. F. *Science* **1998**, *281*, 969–971.

(37) Liu, B.; Zeng, H. C. *J. Am. Chem. Soc.* **2004**, *126*, 8124–8125.

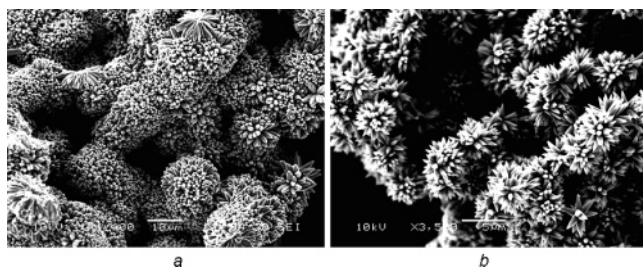


**Figure 3.** Representative SEM images of ZnO derived from the Zn(methylamine)<sub>4</sub>(NTf<sub>2</sub>)<sub>2</sub> precursor at (a) 160 °C and (b) 70 °C.

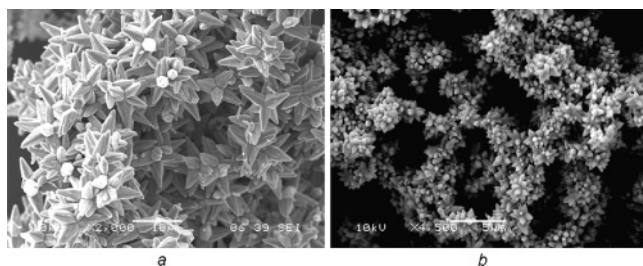


**Figure 4.** Representative SEM images of ZnO from the Zn(propylamine)<sub>4</sub>(NTf<sub>2</sub>)<sub>2</sub> precursor at (a) 160 °C and (b) 70 °C.

Undoubtedly, the ligands of ILs played a key role in the formation of the anisotropic shape of ZnO superstructure in these experiments through selective complexation of crystal surfaces. The primary results indicated that the Zn(II) ILs could serve both as solvents and precursors for ZnO crystals.

**Influence of Reaction Temperature.** The temperature-dependent growth experiments indicate that the reaction temperature has a significant influence on the morphology of ZnO derived from Zn(methylamine)<sub>4</sub>(NTf<sub>2</sub>)<sub>2</sub>, as shown in Figure 3. The ZnO product obtained at 160 °C exhibits a “banana” feature, which is comprised of numerous one-dimensional hexagonal bipyramid microrods. The diameter and length of these microrods were about 1 μm and 5 μm, respectively. However, a flowerlike shape consisting of nanostrips with a tapering feature was observed for the ZnO product obtained at 70 °C. The reaction temperature of 110 °C resulted in formation of the spherical particles made of ZnO nanoplates in Figure 2a. Clearly, the reaction temperature plays a pivotal role in determining the morphology of ZnO derived from the IL using methylamine as complexing ligands. The effect of the reaction temperature on the resulting morphology of the ZnO product derived from Zn(propylamine)<sub>4</sub>(NTf<sub>2</sub>)<sub>2</sub> is, however, more subtle. The main change observed for the Zn(propylamine)<sub>4</sub>(NTf<sub>2</sub>)<sub>2</sub> growth system is that the resulting ZnO crystals become more symmetric with the reaction temperature, as shown in Figure 4. The number of the petals decreases with the reaction temperature. Meanwhile, the petals change to the single-crystal structures from the low-temperature polycrystalline structures made of ZnO nanoparticles as the reaction temperature increases. No significant morphology changes with the reaction temperature were observed for the Zn(octylamine)<sub>4</sub>(NTf<sub>2</sub>)<sub>2</sub> growth system. The products retained the particle structures. Therefore, the increase of alkyl chain length in alkylamine ligands reduces the influence of the reaction temperature on the morphology of the resulting ZnO product.

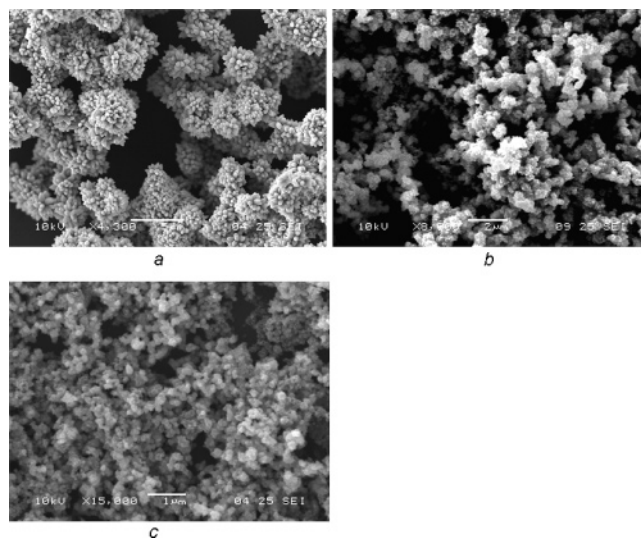


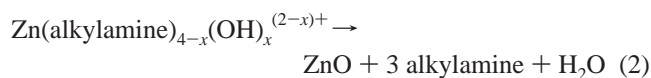
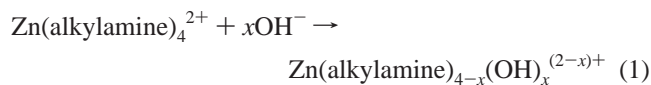
**Figure 5.** Representative SEM images of ZnO from the Zn(propylamine)<sub>4</sub>(NTf<sub>2</sub>)<sub>2</sub> precursor with different hydroxide concentrations (molar ratio) at 110 °C: (a) [OH]/Zn ≈ 1/10, (b) [OH]/Zn ≈ 1/5, and (c) [OH]/Zn ≈ 2/5.

**Influence of Hydroxide Concentration.** The concentration of hydroxide is another important factor for controlling the rate of nucleation. The more hydroxide species will consume the more Zn-containing ionic-liquid solvents through displacement of alkylamine ligands to form Zn(alkylamine)<sub>4-x</sub>(OH)<sub>x</sub><sup>2-x+</sup> under the ionothermal condition. This displacement reaction is directly correlated to the generation of the nucleation centers for ZnO. Therefore, the increase of the hydroxide concentration will significantly influence the morphology of ZnO. Figure 5 shows that the morphology changes from flowerlike ([OH]/Zn ≈ 1/10) to coral structures ([OH]/Zn ≈ 1/5) and eventually to irregular particles ([OH]/Zn ≈ 2/5).

**Influence of Reaction Time.** ILs are well-known for their amphiphilic properties, giving rise to a small interfacial tension.<sup>10</sup> This small interface tension results in high nucleation rates. Accordingly, large-scale uniform products can be generated without the significant interference and competition from Ostwald ripening during the initial nucleation and subsequent growth. To investigate the morphological evolution of the flowerlike ZnO, the Zn(propylamine)<sub>4</sub>(NTf<sub>2</sub>)<sub>2</sub> IL containing a specific amount of hydroxide ([OH]/Zn ≈ 1/10) was heated at 110 °C for various reaction times. A continuous coral structure assembled from ZnO nanoparticles was formed in 30 min (TEM images). The prolongation of the reaction time to 1 h led to the growth of more petals on the coral structure without any visible Ostwald ripening. When the reaction time was further extended to 2 h, the shape of ZnO became perfectly flowerlike. These observations indicate that the reaction time alone could not bring about significant modifications of both structure and morphology of the resulting ZnO.

**Proposed Mechanism.** It is known that the stability constant between hydroxide and zinc is greater than that between alkylamine and zinc.<sup>17</sup> Accordingly, the addition of hydroxide leads to the formation of the mixed Zn(alkylamine)<sub>4-x</sub>(OH)<sub>x</sub><sup>2-x+</sup> complex through the displacement reaction (eq 1). The stability of Zn(alkylamine)<sub>4-x</sub>(OH)<sub>x</sub><sup>2-x+</sup> considerably decreases with the reaction temperature because

of condensation and decomposition of  $\text{Zn}(\text{alkylamine})_{4-x}(\text{OH})_x^{(2-x)+}$  to form ZnO (eq 2).



Decomposing soluble  $\text{Zn}(\text{alkylamine})_{4-x}(\text{OH})_x^{(2-x)+}$  precursors in ILs gave the ZnO product with different morphology depending on the ligands, as shown in Figure 2. The corresponding TEM images showed that the morphology with micrometer sizes was assembled by the secondary aggregation of nanostructures [ $\text{Zn}(\text{C}_n\text{H}_{2n+1}\text{NH}_2)_4(\text{NTf}_2)_2$ : nanostrips ( $n \leq 2$ ); nanoparticles ( $n > 2$ )]. The alkylamine byproduct provides the in situ capping reagent for preventing the ZnO nucleation centers from aggregation during the growth process. Accordingly, the properties of the alkylamine, such as the chain length, can affect the final morphology of ZnO. The long chain alkylamine, such as octylamine, functioned as surfactants, stabilizing ZnO nanoparticles via the minimization of their surface energy and blockage of the ion diffusion. This unique interfacial interaction results in formation of monodispersed nanoparticles, as shown in Figure 2i. On the other hand, the short-chain alkylamine ligands cannot stabilize the monodispersed nanostrips and therefore lead to large-scale continuous morphologies, such as flowers or nanoplates. For example, methylamine only contains one carbon atom and has a low boiling point. Accordingly, the temperature factor could have a significant influence on the product morphological diversity, as shown in Figures 2a and 3. However, with increase of alkyl chain length, the temperature influence should become less visible. This effect can be clearly seen for the systems containing propylamine or butylamine ligands, as shown in Figure 4. The structural differences among the alkylamine ligands used in synthesizing the  $\text{Zn}(\text{alkylamine})_{4-x}(\text{OH})_x^{(2-x)+}$  precursor species can also affect the solvent properties of the resulting ILs and thereby lead to the different morphologies of ZnO products. Accordingly, the stereochemistry associated with the chain length and surface

packing of the alkylamine ligands could also influence the morphology of the resulting ZnO nanostructures. Each of the aforesaid factors plays a specific role in leading the formation of different morphologies of ZnO crystals. We propose that the morphological control of ZnO nanoscale materials results primarily from the temperature and ligands although the combination of different factors determines the final architecture of ZnO crystals. The detailed kinetics and reaction mechanisms of the system presented here are currently under investigation.

## Conclusions

We have successfully demonstrated that the new metal-containing ILs can be utilized as both solvents and metal-oxide precursors for growth of metal-oxide nanostructures. The ZnO materials with various morphologies can be synthesized under the ionothermal condition. The morphologies of ZnO are strongly dependent on the nature of the IL precursor (ligands), providing unique methodologies to control the growth conditions. The versatility of this synthesis method is a major asset: (1) the ability to tune solvent properties via tailoring ligand structures for metal ions and (2) the potential to replace zinc ions with other transition metal ions for the homogeneous nucleation synthesis of other binary and ternary metal oxides. Thus, this new synthesis methodology offers a unique alternative avenue to synthesize metal-oxide and complex metal-oxide nanostructures with tunable morphologies.

**Acknowledgment.** This work was supported by the Office of Basic Energy Sciences, U.S. Department of Energy. The Oak Ridge National Laboratory is managed by UT-Battelle, LLC, for the U.S. DOE under Contract DE-AC05-00OR22725. This research was supported in part by the appointments for H. Zhu to the ORNL Research Associates Program, administered jointly by ORNL and the Oak Ridge Institute for Science and Education. We also acknowledge the ORNL HTML Collaborative High-Temperature Research Laboratory, which provided the facility for the TEM analyses.

**Supporting Information Available:** HRTEM, TEM, and SEM of ZnO obtained with different reaction times. This material is available free of charge via the Internet at <http://pubs.acs.org>.

CM060472Y